atom of a cysteine side chain, which bridges to the adjacent Fe_4S_4 cluster, but no electron density is resolved on the distal side. It is unclear, however, in view of the limited resolution of the diffraction data, whether this observation excludes a bound distal ligand, perhaps a water molecule. A sixth, weak-field ligand would provide the most straightforward explanation of the RR frequencies, although it cannot be excluded that some other protein influence, perhaps a ruffling distortion, might mimic the effect of a sixth ligand on the band positions.

An important observation of the SiR study was that reduction of HP^0 by two successive electrons did not produce a monotonic change in the RR spectra.[15] Rather an intermediate spectrum was detected upon addition of one electron, in which the highest frequency band was higher than in either HP^0 or HP^{2-}. This behavior was interpreted as resulting from the formation of low- or intermediate-spin iron(II) siroheme in the intermediate HP^-, which was then converted to high-spin iron(II) siroheme on addition of a second electron, which reduces the Fe_4S_4 cluster. Since the Mössbauer parameters are inconsistent with low-spin iron(II) siroheme in HP^-, an intermediate spin state was inferred. Intermediate-spin Fe(II) results from a weak or absent axial ligand field. It was suggested that reduction of the Fe(III) in HP^0 weakens or breaks the bond to the bridging ligand, presumably cysteine, leaving intermediate-spin Fe(II). Subsequent reduction of the Fe_4S_4 cluster reforms and/or strengthens the bond to the siroheme Fe(II) because of the additional negative charge on the bridging ligand, producing five-coordinate high-spin Fe(II). Figure 12 strengthens this interpretation by showing that the high-frequency RR spectra of all three oxidation levels, HP^0, HP^-, and HP^{2-}, are accurately modeled by the appropriate OEiBC complex, $(DMSO)_2Fe^{III}$, four-coordinate Fe(II), and 1,2-dimethylimidazole–Fe(II), respectively. The close match of HP^- with the intermediate-spin Fe(II) is especially important in confirming the weakening of the axial siroheme bond to the cluster-bound ligand, an interaction that may play an important role in the mechanism of the concerted six-electron reduction of sulfite by SiR.

Acknowledgment. This work was supported by a grant to T.G.S. from the U.S. Department of Energy (DE-FG02-88ER13876) and by grants to S.H.S. from the National Science Foundation (CHE-8805788) and from the donors of the Petroleum Research Fund, administered by the American Chemical Society.

Contribution from the Department of Chemistry, State University of New York, Stony Brook, New York 11794

Redox Reactions of Mixed-Valence Complexes: Kinetic and Thermodynamic Considerations in the (μ-Pyrazine)((ethylenediaminetetraacetato)ruthenato)pentaammineruthenium Ru^{II},Ru^{II}, Ru^{II},Ru^{III}, and Ru^{III},Ru^{III} Systems

M. S. Ram and Albert Haim*

Received April 3, 1990

The oxidation of the mixed-valence compound M in the title (Ru^{III}(EDTA), $Ru^{II}(NH_3)_5$) by peroxydisulfate proceeds according to the rate law $(a + b[S_2O_8^{2-}])[M]$. The peroxydisulfate-independent term corresponds to slow dissociation of M (to form $Ru^{II}(NH_3)_5pz^{2+}$ (pz = pyrazine) and $Ru^{III}(EDTA)OH_2^-$ (EDTA = ethylenediaminetetraacetate)) and is followed by the rapid reaction of $Ru^{II}(NH_3)_5pz^{2+}$ with peroxydisulfate. The peroxydisulfate-dependent term corresponds to direct reaction between M and $S_2O_8^{2-}$. The reduced form (II, II) of the compound in the title, R, reacts with peroxydisulfate according to biphasic kinetics. The first phase corresponds to oxidation of R to M, and the second phase is the reaction of M with $S_2O_8^{2-}$. On the basis of reactivity patterns for the peroxydisulfate oxidation of pyrazine complexes of $Ru^{II}(NH_3)_5^{2+}$ and of $Ru^{II}(EDTA)^{2-}$, it is suggested that oxidation of R yields, as the primary product of the reaction, $(NH_3)_5Ru^{III}pzRu^{II}(EDTA)^+$, the electronic isomer of the title compound M, which then undergoes rapid intramolecular electron transfer to produce the stable isomer M. The thermodynamic stability of M toward disproportionation, electronic isomerization, and dissociation is discussed on the basis of electronic, electrostatic, and metal $d\pi$–ligand π^* bonding factors.

In the past few years, several research groups have synthesized and studied the electrochemical and spectroscopic properties of mixed-valence transition-metal complexes.[1-4] Our contributions to this subject have emphasized the redox reactivities of hetero- and homobinuclear mixed-valence complexes and their corresponding isovalent states.[5-8] In a continuation of this work, we now focus our attention on the title compound, the pyrazine-bridged heterobinuclear complex M, a class II (trapped-valence)

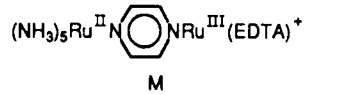

M

mixed-valence compound. (EDTA represents pentadentate ethylenediaminetetraacetate.)[9] The reactions of M with one- and two-electron reagents are reported in the present work. For comparison purposes, we also report some redox reactions of the mononuclear complex $Ru^{II}(EDTA)pz^{2-}$ (pz is pyrazine) and of the completely reduced complex R. In fact, the results obtained with the latter complex proved to be the most interesting.

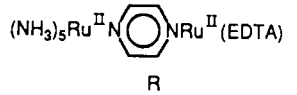

R

Experimental Section

Materials. $Ru^{III}(HEDTA)H_2O{\cdot}4H_2O$ was prepared according to the literature procedure.[10] Trifluoromethanesulfonic acid was purified by distillation under reduced pressure. Lithium trifluoromethanesulfonate was prepared by neutralization of lithium carbonate with CF_3SO_3H. Potassium peroxydisulfate was recrystallized from hot water. House-distilled water was passed through a Barnstead ion-exchange deminer-alizer and then was distilled in a modified, all-glass Corning Model Ag-1b

(1) Creutz, C. *Prog. Inorg. Chem.* **1981**, *30*, 1.
(2) Lay, P. A.; Magnuson, R. H.; Taube, H. *Inorg. Chem.* **1988**, *27*, 2364.
(3) Stebler, A.; Ammeter, J. H.; Furholz, U.; Ludi, A. *Inorg. Chem.* **1984**, *23*, 2764.
(4) Geselowitz, D. A.; Kutner, W.; Meyer, T. J. *Inorg. Chem.* **1986**, *25*, 2015.
(5) Yeh, A.; Haim, A. *J. Am. Chem. Soc.* **1985**, *107*, 369.
(6) Furholz, U.; Haim, A. *J. Phys. Chem.* **1986**, *90*, 3686.
(7) Furholz, U.; Haim, A. *Inorg. Chem.* **1987**, *26*, 3243.
(8) Burewicz, A.; Haim, A. *Inorg. Chem.* **1988**, *27*, 1611.
(9) Creutz, C.; Kroger, P.; Matsubara, T.; Netzel, T. L.; Sutin, N. *J. Am. Chem. Soc.* **1979**, *101*, 5542.
(10) Mukaida, M.; Okuno, H.; Ishimori, T. *Nippon Kagaku Zasshi* **1965**, *86*, 589.

0020-1669/91/1330-1319$02.50/0

apparatus. All other reagents were used as received. The following complexes were available from previous studies: $[Ru^{II}(NH_3)_5pz](PF_6)_2$, $[Ru_2(NH_3)_{10}pz](CF_3SO_3)_5$, $[Ru(NH_3)_5py](PF_6)_2$, $[RuRh(NH_3)_{10}pz](CF_3SO_3)_5$ (pz = pyrazine, py = pyridine).

Preparation of Solutions of Reagents. Solutions of $Ru^{II}(EDTA)pz^{2-}$. Solutions of $Ru^{II}(EDTA)OH_2^{2-}$ were prepared by reduction of $Ru^{III}(EDTA)H_2O^-$ solutions with amalgamated zinc under argon.[11] Typically, (1–2) × 10^{-4} M Ru(III) solutions were prepared in 1.0 × 10^{-2} M, pH 4.8 acetate buffer or 2.5 × 10^{-2} M, pH 5.8 acetate buffer. After reduction, the resulting solution was added slowly via syringe into a degassed solution of pyrazine in 5-fold molar excess with respect to Ru(II). The resulting yellow-orange solutions exhibited a maximum at 463 nm with molar absorption coefficient 1.2 × 10^4 M^{-1} cm^{-1}, in excellent agreement with literature values.[9] Because of their high sensitivity to dioxygen, most solutions of $Ru^{II}(EDTA)pz^{2-}$ were contaminated with the corresponding Ru(III) complex. In particular, for stopped-flow measurements, as much as half of the ruthenium was present as Ru(III).

Solutions of $(NH_3)_5Ru^{II}pzRu^{III}(EDTA)^+$. These solutions were prepared by mixing equimolar solutions (each ~1 × 10^{-4} M) of $Ru^{II}(NH_3)_5pz^{2+}$ and of $Ru^{III}(EDTA)H_2O^-$ at pH 4.8 (1.0 × 10^{-2} M acetate buffer). The mixing was done aerobically since M is not oxygen-sensitive. Because of the low formation constant of M (3 × 10^4 M^{-1}),[11] the pink solutions (wavelength for maximum 520 nm with molar absorption coefficient 1.7 × 10^4 M^{-1} cm^{-1}) always contain free mononuclear species.

Solutions of $(NH_3)_5Ru^{II}pzRu^{II}(EDTA)$. These were prepared by reduction of ~1 × 10^{-4} M solutions of $(NH_3)_5Ru^{II}pzRu^{III}(EDTA)^+$ with amalgamated zinc. The purple solutions (λ_{max} = 544 nm with molar absorption coefficient ~2.5 × 10^4 M^{-1} cm^{-1}) were extremely sensitive to dioxygen.

Solutions of $(EDTA)Ru^{II}pzRu^{II}(EDTA)^{4-}$ and $(EDTA)Ru^{II}pzRu^{III}(EDTA)^{3-}$. The former were prepared by mixing, under strictly anaerobic conditions, solutions of $Ru^{II}(EDTA)OH_2^{2-}$ and of pyrazine such that the final concentrations were 2.0 × 10^{-4} and 1.0 × 10^{-4} M, respectively. All $Ru^{II}Ru^{II}$ are extremely sensitive to dioxygen and were handled routinely under argon in syringes containing several pieces of amalgamated zinc. The purple solutions display an absorption maximum at 544 nm with molar absorption coefficient 2.5 × 10^4 M^{-1} cm^{-1}. Solutions of $(EDTA)Ru^{II}pzRu^{III}(EDTA)^{3-}$ were prepared by mixing, under strictly anaerobic conditions, solutions of $Ru^{II}(EDTA)OH_2^{2-}$, $Ru^{III}(EDTA)OH_2^-$, and pyrazine such that the final concentrations were 1.0 × 10^{-4}, 2.3 × 10^{-4}, and 1.0 × 10^{-4} M, respectively. The pink solutions display an absorption maximum at 528 nm with molar absorption coefficient 1.4 × 10^4 M^{-1} cm^{-1}.

Measurements. Absorption spectra were measured with a Cary 118 spectrophotometer. Kinetic measurements of slow and fast reactions were carried out with Cary 118 and Durrum D-110 instruments, respectively. Data handling and processing of the stopped-flow measurements were described in detail previously.[8,12,13] In most instances first-order kinetics were obeyed and rate constants k_{obsd} were calculated by nonlinear least-squares fitting of A_t to t according to $A_t - A_\infty = (A_0 - A_\infty) \times \exp(-k_{obs}t)$, where A_0, A_t, and A_∞ are the absorbances at time 0, at time t, and at long ($>8t_{1/2}$) times, respectively. Systems that displayed biphasic kinetics were fitted to the equation $A_t - A_\infty = P_1 \exp(-k_1 t) + P_2 \exp(-k_2 t)$ by nonlinear least-squares calculations. pH and cyclic voltammetric measurements were carried out as described previously.[5]

Results

Reactions of $(NH_3)_5Ru^{II}pzRu^{III}(EDTA)^+$. When solutions of $Ru(EDTA)H_2O^-$ and of $Ru(NH_3)_5pz^{2+}$ are mixed, M is produced rapidly according to eq 1.[9] Values of k_1 and k_{-1} are 2.7 × 10^4 M^{-1} s^{-1} and 0.90 s^{-1} at 25 °C and 0.20 M ionic strength.[1] With

$$Ru^{II}(NH_3)_5pz^{2+} + Ru^{III}(EDTA)H_2O^- \underset{k_{-1}}{\overset{k_1}{\rightleftharpoons}} (NH_3)_5Ru^{II}pzRu^{III}(EDTA)^+ + H_2O \quad (1)$$

equimolar concentrations of the mononuclear complexes at ~7 × 10^{-5} M, the yield of M is about 50%, and, therefore, it must be recognized that approximately equal concentrations of $Ru(NH_3)_5pz^{2+}$, $Ru(EDTA)H_2O^-$, and M are present in solution and that equilibration between these species occurs rather rapidly.

Since M is a mixed-valence complex, it can be oxidized and reduced. The oxidation potential of M has been measured[9] and found to be 0.56 V at 25 °C and 0.20 M ionic strength, but the reduction potential has not been reported. Therefore, we carried out cyclic voltammetric studies at 25 °C, pH 4.8 (1.0 × 10^{-2} M acetate buffer), 0.10 M ionic strength ($LiCF_3SO_3$), and ~1 × 10^{-3} M each $Ru(EDTA)OH_2^-$ and $Ru(NH_3)_5pz^{2+}$. Under these conditions, more than 80% yield of M is obtained. The measured potentials, which were found to be reversible and independent of which reagent was in slight excess, are summarized in eq 2, where

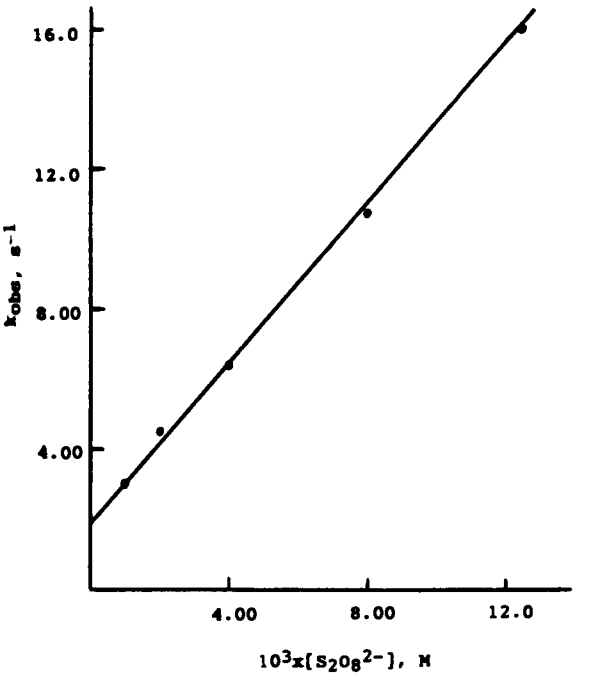

Figure 1. Observed rate constants vs peroxydisulfate concentration for reaction 3: [M] = (1.5–2.0) × 10^{-5} M, pH 4.8 (acetate), ionic strength 0.100 M, 25 °C.

$$(III,III)^{2+} + e^- \xrightarrow{0.57\ V} (III,II)^+ + e^- \xrightarrow{0.21\ V} (II,II) \quad (2)$$

$(III,III)^{2+}$, $(III,II)^+$, and (II,II) represent $(NH_3)_5Ru^{III}pzRu^{III}(EDTA)^{2+}$, compound M, and compound R, respectively. The value we obtained for the first reduction (0.57 V) is in excellent agreement with the reported[9] value (0.56 V).

The characteristic absorption of M at 520 nm disappears when excess peroxydisulfate is added but is regenerated quantitatively when excess ascorbic acid is added. We take the absorbance decrease to be associated with reaction 3. The kinetics of reaction

$$2(NH_3)_5Ru^{II}pzRu^{III}(EDTA)^+ + S_2O_8^{2-} \rightarrow 2(NH_3)_5Ru^{III}pzRu^{III}(EDTA)^{2+} + 2SO_4^{2-} \quad (3)$$

3 at 25 °C, pH 4.28 (5.0 × 10^{-3} M acetate buffer), and 0.10 M ionic strength was studied by measuring the absorbance decrease at 520 nm. The initial concentrations (before mixing in the stopped-flow apparatus) of $Ru(NH_3)_5pz^{2+}$ and $Ru(EDTA)H_2O^-$ were 7.0 × 10^{-5} M, and $S_2O_8^{2-}$ was in excess (1.0 × 10^{-3}–1.29 × 10^{-2} M). Linear plots of ln ($A_t - A_\infty$) vs t were obtained, and the observed first-order rate constants are plotted vs $[S_2O_8^{2-}]$ in Figure 1. A linear least-squares fit of k_{obsd} vs $[S_2O_8^{2-}]$ according to $k_{obsd} = a + b[S_2O_8^{2-}]$ yields values of a = 1.9 ± 0.2 s^{-1} and b = (1.14 ± 0.03) × 10^3 M^{-1} s^{-1}.

Reactions of $(NH_3)_5Ru^{II}pzRu^{II}(EDTA)$. The oxidations of R by $Co^{III}(EDTA)^-$, $Co(bpy)_3^{3+}$, and $S_2O_8^{2-}$ were studied by following the absorbance decreases at 600 nm. For the former two oxidants, only oxidation to M is thermodynamically favorable. With [R] ~ 1 × 10^{-4} M and the oxidant concentration in the range (5–10) × 10^{-4} M, the absorbance decreases were first-order, and the observed rate constants depended linearly on the oxidant concentration. Second-order rate constants for $Co^{III}(bpy)_3^{3+}$ and $Co(EDTA)^-$ were (6.5 ± 0.5) × 10^4 and (4.9 ± 0.1) × 10 M^{-1} s^{-1}, respectively. For the reaction with $S_2O_8^{2-}$, two-electron oxidation is thermodynamically favorable. With $[R]_0$ = 3.8 × 10^{-5}

(11) Matsubara, T.; Creutz, C. *Inorg. Chem.* **1979**, *18*, 1956.
(12) Akhtar, M. J.; Haim, A. *Inorg. Chem.* **1988**, *27*, 1608.
(13) Lee, G.-H.; Della Ciana, L.; Haim, A. *J. Am. Chem. Soc.* **1989**, *111*, 2536.
(14) Olabe, J. A.; Haim, A. *Inorg. Chem.* **1989**, *28*, 3277.

Table I. Kinetics of the Reaction between $(NH_3)_5Ru^{II}pzRu^{II}(EDTA)$ and $S_2O_8^{2-}$ [a]

	k_{obsd}, s^{-1}			k_{obsd}, s^{-1}	
$[S_2O_8^{2-}]$, M	*b*	*c*	$[S_2O_8^{2-}]$, M	*b*	*c*
5.0×10^{-4}	28.2	1.9 (2.4)	2.0×10^{-3}	88	4.5 (4.1)
1.0×10^{-3}		2.8 (3.0)	4.0×10^{-3}	191	

[a] $[(NH_3)_5Ru^{II}pzRu^{II}(EDTA)] = 3.8 \times 10^{-5}$ M; pH 4.8 (5.0×10^{-3} M acetate); ionic strength 0.10 M ($LiCF_3SO_3$); 25 °C. [b] Rapid phase; measurements at 600 nm. [c] Slow phase; measurements at 545 nm.

M and $[S_2O_8^{2-}]_0 = (5.0–40) \times 10^{-3}$ M, biphasic absorbance decreases were observed at 600 and 545 nm. The absorbance changes were larger for the first phase at 600 nm and for the second phase at 545 nm. Therefore, rate constants for the first and second phases were obtained from measurements at 600 and 545 nm, respectively, which are ascribed to reactions 4 and 3,

$$2(NH_3)_5Ru^{II}pzRu^{II}(EDTA) + S_2O_8^{2-} \rightarrow 2(NH_3)_5Ru^{II}pzRu^{III}(EDTA)^{+} + 2SO_4^{2-} \quad (4)$$

respectively. The data at 600 nm were analyzed utilizing a two-exponential fit with the slower exponential fixed at the known value for reaction 3. The data at 545 nm were analyzed utilizing a single-exponential fit, making certain that points were collected following substantial completion of the first phase. The observed rate constants are presented in Table I. The values in parentheses in column 3 are calculated from the equation $k_{obs} = 1.9 + 1.1 \times 10^3[S_2O_8^{2-}]$, $\times 10^3[S_2O_8^{2-}]$, which describes the kinetics of oxidation of M by peroxydisulfate. The measurements of the rapid phase define a second-order rate constant for eq 4 equal to $(2.5 \pm 0.3) \times 10^4$ M^{-1} s^{-1}. The absorbance changes associated with the first phase of the reaction demonstrate that quantitative formation of M obtains in reaction 4. Thus, when a mixture of 1.6×10^{-5} M R and 2.15×10^{-5} M M is oxidized with excess peroxydisulfate, the observed absorbance change at 600 nm for the first stage is 0.26 (2-cm path length). The calculated value for quantitative transformation of R to M is 0.24 (the molar absorbances of R and M at 600 nm are 1.1×10^4 and 3.2×10^3 M^{-1} cm^{-1}, respectively).

Reactions of $Ru^{II}(EDTA)pz^{2-}$. Studies of the reaction of $Ru^{II}(EDTA)pz^{2-}$ with peroxydisulfate proved to be extremely complex. Under ordinary handling conditions, and with peroxydisulfate in excess, the disappearance of $Ru^{II}(EDTA)pz^{2-}$ appeared to be mixed first-order and zero-order. Working with an increased concentration of $Ru^{II}(EDTA)pz^{2-}$ ($\sim 7 \times 10^{-5}$ M) and taking extreme precautions to remove dioxygen could minimize the zero-order component to the last 10% of the reaction, but it could not be eliminated completely. Even under these conditions, reproducibility was no better than ±50%. Similar serious difficulties have been reported[11] in studies of the reaction of $Ru^{II}(EDTA)OH_2^{2-}$ with pyrazine. Since under improved handling conditions, exponential behavior was observed during the first 90% of reaction, the data were treated according to first-order kinetics, and the resulting observed rate constants are plotted in Figure 2 as a function of peroxydisulfate concentration. Variations in pH or concentrations of added pyrazine, EDTA, or $Ru^{III}(EDTA)pz^{-}$ did not appear to affect the rates more than the usual irreproducibility. It will be seen (Figure 2) that at high peroxydisulfate concentration the first-order rate constant reaches a limiting value in the vicinity of 0.3 s^{-1}. A second-order component is not detectable, and thus a direct reaction between $Ru^{II}(EDTA)pz^{2-}$ and 0.020 M peroxydisulfate is rather slow. Assuming that under these conditions the direct reaction has $k_{obs} < 0.3$ s^{-1}, we estimate that the second-order rate constant is <8 M^{-1} s^{-1}.

Additional reactions of the $Ru(EDTA)pz^{2-/-}$ couple with several one-electron redox couples were studied, and the results are presented in Table II. The measurable reactions obeyed good first-order kinetics.

The equilibrium constant for addition of a proton to the free pyrazine N in $Ru(EDTA)pz^{2-}$ was estimated by a spectrophotometric procedure. Addition of acid to a neutral solution of

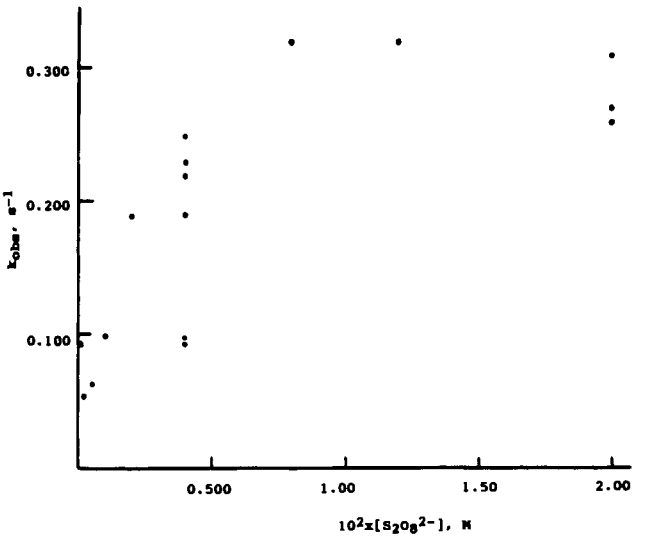

Figure 2. Observed rate constants vs peroxydisulfate concentration for oxidation of $Ru^{II}(EDTA)pz^{2-}$: $[Ru(EDTA)pz^{2-}] = (3.5–7.5) \times 10^{-5}$ M, pH 4.8 or 5.8 (acetate), ionic strength 0.100 M, 25 °C, [pz] = 1.0×10^{-4}–0.100 M, $[Ru^{III}(EDTA)pz^{-}] = (0–3.40) \times 10^{-4}$, [EDTA] = $(0–2.00) \times 10^{-4}$.

Table II. Kinetics of Oxidation of $Ru^{II}(EDTA)pz^{2-}$ by Several Oxidizing Agents[a]

oxidant (concn, M)	k, M^{-1} s^{-1}
$Ru(NH_3)_5py^{3+}$ (1×10^{-3})	$>2 \times 10^5$
$Ru(NH_3)_6^{2+}$ [b] (5×10^{-5})	$>4 \times 10^6$
$Co(EDTA)^{-}$ ($(2.5–5) \times 10^{-3}$)	13 ± 1
$Co(bpy)_3^{3+}$ ($(5–50) \times 10^{-4}$)	$(2.5 \pm 0.2) \times 10^4$

[a] $[Ru(EDTA)pz^{2-}] = (3–7) \times 10^{-5}$ M; pH = 4.8 (5.0×10^{-3} M acetate); ionic strength 0.10 M ($LiCF_3SO_3$); t = 25 °C. [b] This reaction is actually the reduction of $Ru^{III}(EDTA)pz^{-}$ by $Ru^{II}(NH_3)_6^{2+}$.

$Ru^{II}(EDTA)pz^{2-}$ results in a decrease in the absorption at 463 nm, the appearance of a new band at 545 nm, and the development of a clean isosbestic point at 490 nm. Plots of $(A_m - A_B)/(A_A - A_m)$ vs $[H^+]$ at 545 or 463 nm are linear and yield a pK_a of 2.5 for proton dissociation from $Ru(EDTA)pzH^{-}$. A_m, A_A, and A_B are the measured absorbance, the absorbance of the acid form, and the absorbance of the basic form, respectively. Although $Ru(EDTA)pz^{2-}$ has two potential protonation sites, namely, the remote N of pyrazine and an oxygen atom in the dangling carboxylate, the observation of a linear plot indicates that the pK_a values of the two protonation sites are similar, a reasonable result in view of the reported $pK_a = 2.4$ for $Ru(HEDTA)OH_2$, where HEDTA represents pentadentate ethylenediaminetetraacetate with a protonated dangling carboxylate.

Catalysis by $Ru^{II}(NH_3)_5L^{n+}$ (L = pz or $Rh(NH_3)_5pz^{3+}$) of the $Ru^{II}(EDTA)pz^{2-}$–$S_2O_8^{2-}$ Reaction. Addition of micromolar concentrations of $Ru^{II}(NH_3)_5L^{n+}$ (L = pz or $Rh(NH_3)_5pz^{3+}$) to solutions of $Ru^{II}(EDTA)pz^{2-}$ and $S_2O_8^{2-}$ resulted in a dramatic increase in rate and a transition to zero-order kinetics. For example, with $[Ru^{II}(EDTA)pz^{2-}] = 5.0 \times 10^{-5}$ M and $[S_2O_8^{2-}] = 2.0 \times 10^{-3}$ M, addition of 5.0×10^{-6} M $Ru(NH_3)_5pz^{2+}$ decreased the half-life from ~3 s (first order) to ~0.3 s (zero order). The measurements were treated on the basis of zero-order kinetics, and the observed rates are listed in column 3 of Table III. For $Ru^{II}(NH_3)_5pz^{2+}$ as catalyst, rates are approximately first order each in $[S_2O_8^{2-}]$ and $[Ru^{II}(NH_3)_5pz^{2+}]$. For $Ru^{II}Rh^{III}(NH_3)_{10}pz^{5+}$ as catalyst, the reaction is less than first order in $[S_2O_8^{2-}]$, as expected on the basis of the strong ion pair association[7] between $S_2O_8^{2-}$ and the binuclear complex.

Reactions of $Ru_2(EDTA)_2pz^{4-}$ and $Ru_2(EDTA)_2pz^{3-}$. A brief examination of these reactions was carried out. With $(EDTA)Ru^{II}pzRu^{II}(EDTA)^{4-}$ at 1.0×10^{-4} M and $[S_2O_8^{2-}] = (1.0–4.0) \times 10^{-3}$ M, absorbance decreases at 600 nm display biphasic kinetics. For $(EDTA)Ru^{II}pzRu^{III}(EDTA)^{3-}$ under the same conditions, only monophasic kinetics were observed. The second-order

Table III. Kinetics of the Peroxydisulfate Oxidation of $Ru^{II}(EDTA)pz^{2-}$ Catalyzed by $Ru^{II}(NH_3)_5L^{n+}$ (L = pz or $Rh(NH_3)_5pz^{3+}$)[a]

catalyst (concn, M)	$[S_2O_8^{2-}]$, M	rate, M/s obsd[b]	rate, M/s calcd[c]
$Ru^{II}(NH_3)_5pz^{2+}$ (5.0×10^{-6})	5.0×10^{-4}	2.5×10^{-5}	2.4×10^{-5}
$Ru^{II}(NH_3)_5pz^{2+}$ (5.0×10^{-6})	1.0×10^{-3}	5.8×10^{-5}	4.7×10^{-5}
$Ru^{II}(NH_3)_5pz^{2+}$ (5.0×10^{-6})	2.0×10^{-3}	1.0×10^{-4}	8.6×10^{-5}
$Ru^{II}(NH_3)_5pz^{2+}$ (1.0×10^{-5})	1.0×10^{-3}	1.5×10^{-4}	1.1×10^{-4}
$(NH_3)_5Ru^{II}pzRh^{III}(NH_3)_5^{5+}$ (4.8×10^{-6})	5.0×10^{-4}	7.3×10^{-5}	9.2×10^{-5}
$(NH_3)_5Ru^{II}pzRh^{III}(NH_3)_5^{5+}$ (4.8×10^{-6})	2.0×10^{-3}	1.7×10^{-4}	2.9×10^{-4}

[a] $[Ru^{II}(EDTA)pz^{2-}] = (3\text{–}6) \times 10^{-5}$ M; pH 4.8 (5.0×10^{-3} M acetate); ionic strength 0.10 M ($LiCF_3SO_3$); t = 25.0 °C. [b] Calculated from the slope of the linear absorbance at 463 nm vs t measurements as slope/ϵl, where ϵ 1.1×10^4 M^{-1} cm^{-1} and l = 2 cm. [c] See ref 21.

Table IV. Rate Constants for Oxidation of Ruthenium(II) Complexes by Peroxydisulfate[a]

complex	k, M^{-1} s^{-1}	$E°$, V	$k/Q_{IP}K^{1/2}$ s^{-1}
$Ru^{II}(NH_3)_5pz^{2+}$	3.9×10^3	0.52	5.6×10^{-6}
$Ru^{II}(EDTA)pz^{2-}$	<8	0.24	$<2 \times 10^{-9}$
$(EDTA)Ru^{II}pzRu^{II}(EDTA)^{4-}$	6.1×10^{2}[b]	0.18	3.5×10^{-9}
$(EDTA)Ru^{II}pzRu^{III}(EDTA)^{3-}$	26	0.32	9.8×10^{-9}
$(NH_3)_5Ru^{II}pzRu^{III}(EDTA)^{+}$	5.5×10^2	0.57	2.4×10^{-6}
$(NH_3)_5Ru^{III}pzRu^{II}(EDTA)^{+}$	1.4×10^{6}[c]	0.37[c]	1.2×10^{-4}
$(NH_3)_5Ru^{II}pzRu^{II}(EDTA)$	2.5×10^4	0.21	1.7×10^{-7}[d], 4.2×10^{-6}[e]

[a] At t = 25 °C and ionic strength 0.10 M. [b] Corrected for the statistical factor of 2. [c] See text. [d] Oxidation of Ru(II) center bound to EDTA. [e] Oxidation of Ru(II) center bound to NH_3.

rate constants for the $S_2O_8^{2-}$–$Ru_2pz(EDTA)_2^{4-}$ and $S_2O_8^{2-}$–$Ru_2pz(EDTA)_2^{3-}$ reactions are $(1.2 \pm 0.2) \times 10^3$ M^{-1} s^{-1} and 26 ± 3 M^{-1} s^{-1}, respectively.

Discussion

Mechanistic Considerations. Rate constants for the reactions of several pyrazine complexes of the pentaammineruthenium(II) and ethylenediaminetetraacetatoruthenate(II) moieties are listed in Table IV. For the mononuclear complexes $Ru^{II}(NH_3)_5pz^{2+}$ and $Ru^{II}(EDTA)pz^{2-}$, as well as for the binuclear complexes $(EDTA)Ru^{II}pzRu^{II}(EDTA)^{4-}$ and $(EDTA)Ru^{II}pzRu^{III}(EDTA)^{3-}$ where the metal centers are equivalent,[9,15] the site that loses an electron is perfectly well-defined: it is the single ruthenium(II) center for the mononuclear complexes or one of a pair of equivalent ruthenium centers for the binuclear complexes. However, for the binuclear complexes $(NH_3)_5Ru^{II}pzRu^{II}(EDTA)$ and $(NH_3)_5Ru^{II}pzRu^{III}(EDTA)^{+}$, where the ruthenium centers are not equivalent, there are subtle mechanistic questions. For the former complex, although the thermodynamically favored site of oxidation is the ruthenium(II) center bound to $EDTA^{4-}$, there is no assurance that it will be kinetically favored as well.[5] In other words, is M the kinetically controlled oxidation product of R (as well as the thermodynamically controlled product), or is the unstable electronic isomer of M, M′, produced as the primary

$$(NH_3)_5Ru^{III}pzRu^{II}(EDTA)^{+}$$
M′

product of the oxidation by peroxydisulfate, with M′, in a subsequent very fast[9] intramolecular electron-transfer process, then yielding the stable isomer M? For $(NH_3)_5Ru^{II}pzRu^{III}(EDTA)^{+}$ a somewhat different question arises.[14] Is M the reactive species, or is M′, formed from M in a rapid preequilibrium, the actual species that undergoes oxidation by peroxydisulfate? In order to answer these questions, we first inquire into the intrinsic (e.g., self-exchange) reactivities of $Ru^{II}(EDTA)pz^{2-}$ and $Ru^{II}(NH_3)_5pz^{2+}$ complexes toward oxidation. The self-exchange rate constant for the $Ru(NH_3)_5pz^{3+/2+}$ couple has been estimated[6] at 1.4×10^4 M^{-1} s^{-1}. An estimate of the self-exchange rate constant for the Ru(EDTA)$pz^{-/2-}$ couple can be obtained from the measured cross reactions with $Co(EDTA)^-$ and $Co(bpy)_3^{3+}$ through the utilization of the Marcus relationship corrected for electrostatics.[16] The values obtained are 8.3×10^5 and 13×10^5 M^{-1} s^{-1}, respectively. Before the self-exchange rate constants for $Ru(NH_3)_5pz^{3+/2+}$ and Ru(EDTA)$pz^{-/2-}$ can be compared, they have to be corrected for the difference in the charges of the corresponding reactants. The correction was carried out by utilization of the ion pair model[16] and yielded values of the self-exchange rate constants within the precursor complexes of $\sim 2 \times 10^5$ and $\sim 8 \times 10^5$ s^{-1} for the $Ru(NH_3)_5pz^{3+/2+}$ and Ru(EDTA)$pz^{-/2-}$ couples, respectively. Because of the approximations involved, we take the intrinsic reactivities of the ammine and EDTA couples to be essentially equal to each other.[18] Consider next the relative reactivities of $Ru^{II}(EDTA)$–pz and $Ru^{II}(NH_3)_5$–pz complexes toward peroxydisulfate. In order to correct for the differences in the reduction potentials and in the charges of the various complexes, we divide the measured rate constants (column 3 of Table IV) by Q_{IP}, the ion pair formation constant[7] between the complex and $S_2O_8^{2-}$, and by $K^{1/2}$, where K is the equilibrium constant for the one-electron oxidation of the complex by $S_2O_8^{2-}$.

$$Q_{IP} = \frac{4\pi Na^3}{3000} \exp(-w/RT)$$

$$w = \frac{z_A z_B e^2}{Da(1 + \beta a \mu^{1/2})} = \frac{w_0}{1 + \beta a \mu^{1/2}}$$

a is the distance between the metal centers (taken as equal to the sum of the radii r_A and r_B of the complexes), z_A and z_B are the charges of the ions, D is the static dielectric constant of water, β is $(8\pi Ne^2/1000DkT)^{1/2}$, and μ is the ionic strength. The one-electron reduction of $S_2O_8^{2-}$ produces a sulfate ion and a sulfate radical ion and corresponds to a reduction potential of 1.45 V.[17] According to this treatment (column 4 of Table IV), the corrected reactivities of $Ru^{II}(NH_3)_5$–pz and $Ru^{II}(EDTA)$–pz complexes are of the order of $\sim 5 \times 10^{-6}$ and $\sim 5 \times 10^{-9}$ $M^{1/2}$ s^{-1}, respectively.

Now we examine the peroxydisulfate oxidations of M and R. Consider first the oxidation of M, which proceeds according to the rate law $(a + b[S_2O_8^{2-}])[M]$. The mechanism proposed to

Scheme I

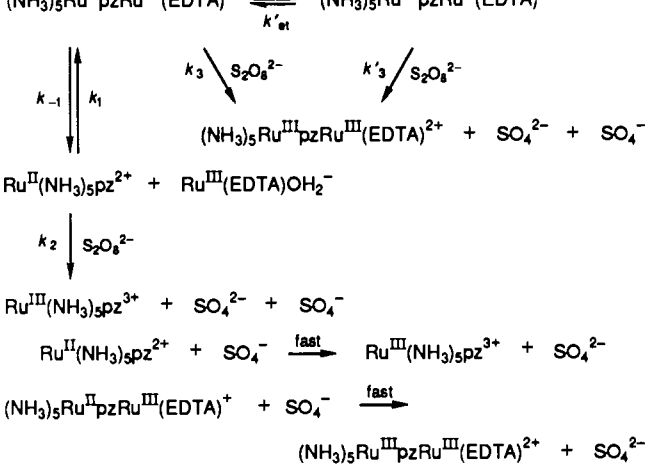

(15) Although (EDTA)Ru(pz)Ru(EDTA)$^{3-}$ is best formulated[9] as a class II complex, intramolecular transfer is rapid[1] compared to reaction with $S_2O_8^{2-}$, and therefore the two ruthenium centers are equivalent in the time scale of the experiment.

(16) Brown, G. M.; Sutin, N. *J. Am. Chem. Soc.* **1979**, *101*, 883.
(17) Stanbury, D. *Adv. Inorg. Chem.* **1989**, *33*, 70.
(18) Another example of equal reactivities for ammine and EDTA couples pertains to the $Co(NH_3)_6^{3+/2+}$ and $Co(EDTA)^{-/2-}$ systems.[19,20]
(19) Im, Y. A.; Busch, D. H. *J. Am. Chem. Soc.* **1961**, *83*, 3357.
(20) Geselowitz, D.; Taube, H. *Adv. Inorg. Bioinorg. Mech.* **1982**, *1*, 391.

account for the observed two-term rate law is depicted in Scheme I. According to the proposed scheme, the rate law is given by eq 5 provided that $k_2[S_2O_8^{2-}] > k_1[Ru^{III}(EDTA)OH_2^-]$, a con-

$$\frac{-1}{2}\frac{d[M]}{dt} = k_{-1}[M] + \left(k_3 + \frac{k_{et}}{k'_{et}}k'_3\right)[S_2O_8^{2-}][M] \quad (5)$$

dition met since $k_2[S_2O_8^{2-}] = 3.9$–$50\ s^{-1}$ and $k_1[Ru^{III}(EDTA)OH_2^-] = 0.2\ s^{-1}$. From the measured values of a and b, we calculate $k_{-1} = 0.95\ s^{-1}$ and $k_3 + (k_{et}/k'_{et})k'_3 = 5.5 \times 10^2\ M^{-1}\ s^{-1}$. The value of k_{-1} obtained from the measurements of the reaction of M with peroxydisulfate ($0.95\ s^{-1}$) is in agreement with the value ($0.90\ s^{-1}$) measured[1] directly. The agreement provides strong support for the proposed interpretation. Two limiting conditions can be envisaged for the peroxydisulfate-dependent pathway. If M′ is unreactive, then $k_3 = 5.5 \times 10^2\ M^{-1}\ s^{-1}$. Alternatively, if M is unreactive, then $(k_{et}/k'_{et})k'_3 = 5.5 \times 10^2\ M^{-1}\ s^{-1}$. The value of k_{et}/k'_{et} can be estimated from the following redox cycle.

$$(NH_3)_5Ru^{II}pzRu^{III}(EDTA)^+ \underset{k_{-et}}{\overset{k_{et}}{\rightleftharpoons}} (NH_3)_5Ru^{III}pzRu^{II}(EDTA)^+ \quad (6)$$

$$-E_1^\circ \qquad E_2^\circ$$

$$(NH_3)_5Ru^{III}pzRu^{III}(EDTA)^{2+} + e^-$$

We have measured $E^\circ_1 = 0.57$ V, and E°_2 can be estimated at 0.37 V from the known[9] value for the $(NH_3)_5Rh^{III}pzRu^{III/II}(EDTA)^{2+/+}$ couple. Therefore, $k_{et}/k'_{et} = 4.1 \times 10^{-4}$ and $k'_3 = 1.4 \times 10^6\ M^{-1}\ s^{-1}$. We now turn to the question as to whether M or M′ (or both) is the reactive species. If it is M, then the correction to k_3 for charge and free energy change yields $k_3/Q_{IP}K^{1/2} = 2.4 \times 10^{-6}\ M^{-1/2}\ s^{-1}$. Alternatively, if M′ is the reactive species, then the analogous correction to k'_3 yields $k'_3/Q_{IP}K^{1/2} = 1.2 \times 10^{-4}\ M^{-1/2}\ s^{-1}$. The former value falls nicely in the range of values characteristic of oxidation of a $Ru^{II}(NH_3)_5$–pz site, whereas the latter value is 5 orders of magnitude off the range of values characteristic of oxidation of a $Ru^{II}(EDTA)$–pz site. On this basis, we infer that M is not only the dominant species but the reactive species as well. This situation is opposite that previously[14] observed for the peroxydisulfate oxidation of $(NC)_5Fe(BPA)Ru(NH_3)_5$ (BPA = 1,2-bis(4-pyridiyl)ethane), where the dominant species is the Fe^{II}–Ru^{III} complex but the reactive species is the Fe^{III}–Ru^{II} complex. The reason for the different behavior lies in the much higher rate discrimination between $Ru^{II}(NH_3)_5$ and $Fe^{II}(CN)_5$ centers (a factor of $\sim 10^3$), as well as in the easier accessibility of the unstable electronic isomer in the Ru–Fe system ($k_{et}/k'_{et} = 2.9 \times 10^{-3}$) as compared to the $Ru(NH_3)_5$–Ru(EDTA) system ($k_{et}/k'_{et} = 4.1 \times 10^{-4}$).

Consider now the oxidation of R. If the electron is removed from the $Ru^{II}(EDTA)$ site, as would be the case if the thermodynamically and kinetically controlled products were the same, the corrected rate constant has a value of $1.7 \times 10^{-7}\ M^{1/2}\ s^{-1}$, in poor agreement with values of ca. 10^{-9} characteristic of oxidation of a $Ru^{II}(EDTA)$–pz center. On this basis, we infer that direct oxidation of the $Ru^{II}(EDTA)$–pz site does not occur and suggest, instead, that the mechanism embodied in eqs 7 and 8 is operative.

$$(NH_3)_5Ru^{II}pzRu^{II}(EDTA) + S_2O_8^{2-} \xrightarrow{k_7} (NH_3)_5Ru^{III}pzRu^{II}(EDTA) + SO_4^{2-} + SO_4^- \quad (7)$$

$$(NH_3)_5Ru^{III}pzRu^{II}(EDTA)^+ \xrightarrow{k'_{et}} (NH_3)_5Ru^{II}pzRu^{III}(EDTA)^+ \quad (8)$$

In the proposed sequence, eq 7 is rate-determining and yields the unstable electronic isomer of M. This is followed by the very rapid ($k'_{et} = 8 \times 10^9\ s^{-1}$)[9] intramolecular electron-transfer reaction in eq 8. We then correct k_7 for the free energy change associated with eq 7 using the reduction potential of M′ to R obtained from the following thermodynamic cycle.

$$(NH_3)_5Ru^{III}pzRu^{II}(EDTA)^+ + e^- \xrightarrow{E_3^\circ} (NH_3)_5Ru^{II}pzRu^{II}(EDTA)$$

$$E_4^\circ \qquad E_5^\circ$$

$$(NH_3)_5Ru^{II}pzRu^{III}(EDTA)^+ + e^-$$

E°_4 was estimated above and is equal to 0.20 V, and E°_5 was measured in the present work (0.21 V). Therefore, $E^\circ_3 = 0.41$ V, a reasonable value when it is recognized that addition of a π-donating metal center to the remote N of $Ru^{III}(NH_3)_5pz^{3+}$ results in a decrease in the reduction potential of the latter. For example, the reduction potentials of the $Ru(NH_3)pz^{3+/2+}$ and $Ru_2(NH_3)_{10}pz^{5+/4+}$ couples are 0.52 and 0.40 V, respectively. With $E^\circ_3 = 0.41$ V, we now correct k_3 for free energy changes and for electrostatics and we obtain $k_3/Q_{IP}K^{1/2} = 4.2 \times 10^{-6}\ M^{1/2}\ s^{-1}$, a value within the range of values characteristic of oxidation of a $Ru^{II}(NH_3)_5pz$ site. This agreement provides strong support for the proposed interpretation.

The mechanism given in eqs 7 and 8 represents a form of intramolecular assistance of the oxidation of the $Ru^{II}(EDTA)$ center by $Ru^{II}(NH_3)_5$. The process is not truly catalytic because the "catalyst" is the reactant itself, which, to be sure, is consumed during reaction. A true case of catalysis, but intermolecular, was found for the peroxydisulfate oxidation of $Ru^{II}(EDTA)pz^{2-}$ in the presence of $Ru^{II}(NH_3)_5pz^{2+}$ or $(NH_3)_5Ru^{II}pzRh^{III}(NH_3)_5^{5+}$. The observed zero-order kinetics are accommodated by the reaction sequence given by eqs 9–11 (L = pz or $Rh^{III}(NH_3)_5pz^{3+}$). Pro-

$$Ru^{II}(NH_3)_5L^{n+} + S_2O_8^{2-} \xrightarrow{k_9} Ru^{III}(NH_3)_5L^{(n+1)+} + SO_4^{2-} + SO_4^- \quad \text{slow} \quad (9)$$

$$Ru^{II}(EDTA)pz^{2-} + Ru^{III}(NH_3)_5L^{(n+1)+} \rightarrow Ru^{III}(EDTA)pz^- + Ru^{II}(NH_3)_5L^{n+} \quad \text{fast} \quad (10)$$

$$Ru^{II}(EDTA)pz^{2-} + SO_4^- \rightarrow Ru^{III}(EDTA)pz^- + SO_4^{2-} \quad \text{fast} \quad (11)$$

vided that reaction 10 is fast and favorable ($\Delta E = 0.28$ or 0.51 V), the initial and steady-state concentrations of the $Ru(NH_3)_5L^{n+}$ catalyst are equal within 2% throughout 90% of the reaction, and the zero-order rate of disappearance of $Ru^{II}(EDTA)pz^{2-}$ is $2k_9[Ru(NH_3)_5L^{n+}][S_2O_8^{2-}]$. In addition there is a contribution of the uncatalyzed path for the $Ru^{II}(EDTA)pz^{2-}$–$S_2O_8^{2-}$ reaction (Figure 1). Observed and calculated[21] rates are listed in columns 3 and 4 of Table III. Although the agreement is not spectacular, it is clear that the main features of the catalytic process are well described by eqs 9–11.

A reason for the discrepancies between observed and calculated values in Table III relates to the irreproducibility of the $Ru^{II}(EDTA)pz^{2-}$–$S_2O_8^{2-}$ reaction. Within a high uncertainty, it appears that the reaction rate becomes independent of $[S_2O_8^{2-}]$ above 0.01 M and reaches a value of $\sim 0.3\ s^{-1}$. This limiting rate cannot be loss of pyrazine from $Ru^{II}(EDTA)pz^{2-}$, a process that is known[11] to be several orders of magnitude slower. However, a similar rate ($0.34\ s^{-1}$) was measured for the disappearance of $Ru^{II}(EDTA)pz^{2-}$ when a large excess of acetonitrile (1.0 M) was added to $Ru^{II}(EDTA)pz^{2-}$ solutions. We have no satisfactory explanation for our observation but note that serious difficulties and irreproducible results were also reported[11] in studies of the formation of $Ru^{II}(EDTA)pz^{2-}$ from $Ru^{II}(EDTA)OH_2^{2-}$ and pyrazine.

It is noteworthy that $Ru^{II}(EDTA)pz^{2-}$ reacts with $S_2O_8^{2-}$ at a rate slower than predicted on the basis of the electrostatically corrected Marcus relationship. With a rate constant for self-exchange[7] in the $S_2O_8^{2-}/SO_4^{2-},SO_4^-$ couple of $\sim 4 \times 10^{-18}\ M^{-1}\ s^{-1}$, the rate constant for the $Ru^{II}(EDTA)pz^{2-}$–$S_2O_8^{2-}$ reaction

(21) The mechanism represented by eqs 9–11 and a contribution of the $Ru^{II}(EDTA)pz^{2-}$–$S_2O_8^{2-}$ reaction equal to the measured value (Figure 1) was integrated numerically by utilizing the previously measured[7] values of k_9. The concentration of $Ru^{II}(EDTA)pz^{2-}$ was found to decrease linearly with time, and the corresponding rate of disappearance was calculated and is listed in Table III.

is calculated as 2.4×10^3 M^{-1} s^{-1}, compared with the observed value <8 M^{-1} s^{-1}. In contrast, for the $Ru^{II}(NH_3)_5pz^{2+}$–$S_2O_8^{2-}$ reaction, there is good agreement between experimental (3.9×10^3 M^{-1} s^{-1}) and calculated (3.2×10^3 M^{-1} s^{-1}) values. We have no satisfactory explanation for the discrepancy but note that, for the $Ru^{II}(EDTA)pz^{2-}$–$S_2O_8^{2-}$ reaction, the reactants have like charges. If under these circumstances close approach of the reactants is precluded, coupling of the orbitals involved may be diminished and the reaction may be occurring in the nonadiabatic regime.

Thermodynamic Considerations. Consider three reactions of the mixed valence complex M: disproportionation to form the isovalent states, intramolecular electron transfer to the unstable electronic isomer M′, and dissociation into the component mononuclear complexes.

The equilibrium constant for reaction 12, calculated from the appropriate redox potentials, is 7.9×10^{-7} and, therefore, the additional stability of M with respect to the isovalent states is 4.2 kcal/mol. Among the possible factors that contribute to the

$$2(NH_3)_5Ru^{II}pzRu^{III}pz(EDTA)^+ \rightleftharpoons (NH_3)_5Ru^{II}pzRu^{II}(EDTA) + (NH_3)_5Ru^{III}pzRu^{III}(EDTA)^{2+} \quad (12)$$

stabilization,[5,22,23] we will consider electronic delocalization associated with the mixed-valence species, an electrostatic factor associated with the net charges of the moieties that make up the binuclear complexes, and metal to ligand π-bonding effects.

The contribution of electronic delocalization[22] to the stability can be calculated as $\alpha^2\nu_{max}$, where α^2 is defined in eq 13. ϵ_{max}

$$\alpha^2 = 4.24 \times 10^{-4}\epsilon_{max}\,\Delta\nu_{1/2}/\nu_{max}d^2 \quad (13)$$

and ν_{max} are the wavenumber and molar absorbance, respectively, of the intervalence absorption, d is the distance between metal centers, and $\Delta\nu_{1/2}$ is the band width at half-intensity. From the reported values of ϵ_{max}, ν_{max}, and $\Delta\nu_{1/2}$,[9] we calculate $\alpha = 3.2 \times 10^{-2}$ and $\alpha^2\nu_{max} = 0.03$ kcal/mol. It is seen that the contribution of resonance stabilization is negligible, a not surprising result since the system is best described as possessing trapped valences.[9] Unlike the case for the complexes $Ru_2(NH_3)_{10}pz^{5+}$ and $(NH_3)_5Ru(pz)Fe(CN)_5$,[5,23] where the electrostatic factor favors the mixed-valence state,[24] this factor for M destabilizes the mixed-valence state with respect to the isovalent states: the electrostatic attractions in reactant and products are $2 \times 1 \times 2 = 4$ and $3 \times 1 + 2 \times 2 = 7$, respectively. The decreased stability, estimated from the appropriate ion pair formation constants, amounts to ~0.5 kcal/mol. Therefore, there is need to account for a 4.7 kcal/mol increased stability of M with respect to the isovalent states. Most likely this comes from $d\pi$–π^* interactions.[23] For the isovalent species with oxidation states +3,+3, there is no back-bonding stabilization. For the isovalent species with oxidation states +2,+2, the metal centers as π bases compete for the π acidity of the pyrazine bridging ligand. In contrast, for the mixed-valence compound, the inductive effect of the Ru(III) center coordinated to the pyrazine increases its π acidity and thus stabilizes the Ru^{II}–$pzRu^{III}$ interaction. This is confirmed by recognizing that coordination of $Ru^{III}(EDTA)^-$ to the remote N of $Ru^{II}(NH_3)_5pz^{2+}$ results in a shift of the Ru(II) $d\pi \rightarrow pz\ \pi^*$ MLCT transition to lower energy (472–520 nm).

An alternate and instructive approach to rationalize the stability of M with respect to the isovalent states makes use of the thermodynamic cycle in Scheme II. Free energy changes for the formation of a variety of Ru(III)–pyrazine complexes are tabulated in Table V. Some values have been taken from the literature, and others have been calculated from measured equilibrium constants and measured reduction potentials. It will be seen that

Scheme II

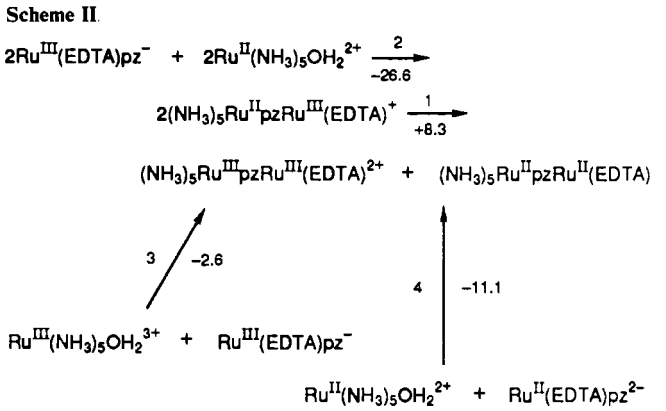

Table V. Free Energy Changes for the Formation of Ruthenium–Pyrazine Complexes at 25 °C and Ionic Strength 0.10 M

reaction	$-\Delta G°$, kcal/mol	ref
$Ru^{II}(EDTA)OH_2^{2-}$ + pz	11.2	11
$Ru^{III}(EDTA)OH_2^-$ + pz	5.4	11
$Ru^{II}(NH_3)_5OH_2^{2+}$ + pz	12.6	25
$Ru^{III}(NH_3)_5OH_2^{3+}$ + pz	3.0	25
$Ru^{II}(EDTA)OH_2^{2-}$ + $Ru^{II}(NH_3)_5pz^{2+}$	11.1	this work
$Ru^{II}(EDTA)OH_2^{2-}$ + $Ru^{III}(NH_3)_5pz^{3+}$	13.7,[a] 18.3[b]	this work
$Ru^{III}(EDTA)OH_2^-$ + $Ru^{II}(NH_3)_5pz^{2+}$	1.5,[a] 6.1[b]	11
$Ru^{III}(EDTA)OH_2^-$ + $Ru^{III}(NH_3)_5pz^{3+}$	5.0	this work
$Ru^{II}(NH_3)_5OH_2^{2+}$ + $Ru^{II}(EDTA)pz^{2-}$	12.5	this work
$Ru^{II}(NH_3)_5OH_2^{2+}$ + $Ru^{III}(EDTA)pz^-$	13.3[b]	this work
$Ru^{III}(NH_3)_5OH_2^{3+}$ + $Ru^{III}(EDTA)pz^{2-}$	2.6	this work
$Ru^{III}(NH_3)_5OH_2^{3+}$ + $Ru^{II}(EDTA)pz^{2-}$	5.5,[a] 10.1[b]	this work

[a] The product is $(NH_3)_5Ru^{III}pzRu^{II}(EDTA)^+$. [b] The product is $(NH_3)_5Ru^{II}pzRu^{III}(EDTA)^+$.

step 1 in Scheme II is uphill by 8.3 kcal. Most of this can be ascribed to stabilization of both moles of reactants by back-bonding (−13.2 kcal/mol, step 2 of Scheme II), whereas only 1 mol of product benefits from that stabilization: values of $\Delta G°$ for steps 3 and 4 of Scheme II are −2.6 and −11.1 kcal, respectively. Evidently, the loss of back-bonding upon oxidation of Ru(II)–pz to Ru(III)–pz is the dominant factor in determining the stability of the mixed-valence complex with respect to disproportionation.

Next we examine the stability of M with respect to its electronic isomer M′, eq 6. The free energy change for eq 6, calculated from the equilibrium constant estimated above, is 4.6 kcal/mol. An electrostatic factor contributes to the difference in stability between M and M′. Note the M is made up of +2,−1 moieties whereas M′ consists of +3,−2 moieties. The difference in stabilities, estimated from ion pair formation constants, amounts to 1.2 kcal/mol in favor of isomer M′. Another way of estimating the electrostatic contribution to $\Delta G°$ for eq 6 consists of assessing the increased stability of Ru(II) in $Ru^{II}(NH_3)_5pz^{2+}$ attending coordination of the remote N by $Ru^{III}(EDTA)^-$ and the increased stability of Ru(II) in $Ru^{II}(EDTA)pz^{2-}$ attending coordination of the remote N by $Ru^{III}(NH_3)_5^{3+}$. The stabilization amounts to 0.08 V in the former case ($E°$ for oxidation of $Ru^{II}(NH_3)_5pz^{2+}$ and $(NH_3)_5Ru^{II}pzRu^{III}(EDTA)^+$ are −0.49 and −0.57 V, respectively) and to 0.13 V in the latter ($E°$ for oxidation of $Ru^{II}(EDTA)pz^{2-}$ and $(NH_3)_5Ru^{III}pzRu^{II}(EDTA)^+$ are −0.24 and −0.37 V, respectively). The difference in stabilities is 0.13–0.05 = 0.08 V or 1.2 kcal in favor of M, in excellent agreement with the value estimated above from ion pair formation constants. Evidently, the electrostatic factor does not favor the more stable isomer. The origin of the stability of M as compared to M′ can be ascertained by examining the thermodynamic cycle in Scheme III. The formation of mononuclear and binuclear complexes (first and last steps in Scheme III) does not favor one or the other of the isomers by a significant amount (−9.1 kcal for M vs −10.9 kcal for M′). The difference in stability between isomers is associated mainly with the middle step in Scheme III: $Ru^{III}(NH_3)_5pz^{3+}$ is a considerably stronger oxidant (0.52 V) than $Ru^{III}(EDTA)pz^-$ (0.24 V). The increased stabilization of Ru(II)

(22) Richardson, D. E.; Taube, H. *J. Am. Chem. Soc.* **1983**, *105*, 40.
(23) Sutton, J. E.; Taube, H. *Inorg. Chem.* **1981**, *20*, 1.
(24) For the former complex the electrostatic repulsions are $2 \times 2 \times 3 = 12$ and $3 \times 3 + 2 \times 2 = 13$ for reactant and products, respectively. For the latter complex the electrostatic attractions are $2 \times 3 \times 3 = 18$ and $2 \times 3 + 3 \times 2 = 12$, respectively.

Scheme III

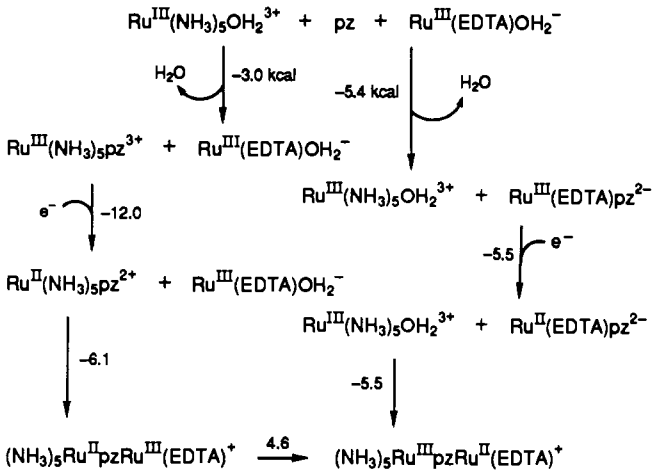

in the ammine system as compared to that in the EDTA system has been ascribed[1] to an increased interaction between the Ru(II) πd and L π^* orbitals.

Finally, we examine the dissociation of M into its component mononuclear units (reverse of eq 1 or eq 14). Table V shows that dissociation of M via rupture of the $Ru^{III}(EDTA)$–pz bond is

$$(NH_3)_5Ru^{II}pzRu^{III}(EDTA)^+ + H_2O \rightleftharpoons Ru^{II}(NH_3)_5pz^{2+} + Ru^{III}(EDTA)OH_2^- \quad (14)$$

considerably more favorable than dissociation via the alternate $Ru^{II}(NH_3)_5$–pz bond rupture mode (ΔG° values of 6.1 and 13.2 kcal/mol, respectively). This results from the substantial stabilization of Ru(II)–pz bonds via Ru(II) dπ–L π^* back-bonding. Free energy changes associated with rupture of a Ru(II)–pz bond fall in the range 11.1–13.3 kcal/mol, whereas free energy changes associated with Ru(III)–pz bond-breaking fall in the range 2.6–6.1 kcal/mol. It is noteworthy that the formation of $Ru^{III}(EDTA)$–pz complexes is 1.3–2.4 kcal more exoergonic than the formation of the corresponding $Ru^{III}(NH_3)_5$–pz complexes. A similar trend is seen for the formation of pyridine and isonicotinamide complexes.[11,25,26] Presumably, Ru(III)–pz back-bonding is practically nonexistent for $Ru^{III}(NH_3)_5^{3+}$, whereas for $Ru^{III}(EDTA)^-$, with the accumulation of negative charge on the ruthenium center, its π basicity is not negligible and is reflected in its higher affinity, compared to that of $Ru^{III}(NH_3)_5^{3+}$, toward the π acidic nitrogen heterocycles.

(25) Wishart, J. F.; Taube, H.; Breslauer, K. J.; Isied, S. S. *Inorg. Chem.* **1984**, *23*, 2997.
(26) ΔG° values for formation of $Ru^{III}(NH_3)_5$–L and $Ru^{III}(EDTA)$–L complexes are: L = pyridine, −4.7 and −6.8 kcal/mol; L = isonicotinamide, −4.5 and −5.6 kcal/mol.

Contribution from the Departments of Chemistry, Southern Methodist University, Dallas, Texas 75275, and The University of Texas at Austin, Austin, Texas 78712

The First Phosphorus Closo Complex of a Dicarborane System: Synthesis and Characterization of 1-[2,4,6-Tris(*tert*-butyl)phenyl]-2,3-bis(trimethylsilyl)-2,3-dicarba-1-phospha-*closo*-heptaborane

Narayan S. Hosmane,*,† Kai-Juan Lu,† Alan H. Cowley,*,‡ and Miguel A. Mardones‡

Received August 24, 1990

The reaction between the $Na^+(THF)Li^+[2,3\text{-}(SiMe_3)_2C_2B_4H_4]^{2-}$ double salt and 2,4,6-$(t\text{-}Bu)_3C_6H_2PCl_2$ in a molar ratio of 1:1 in dry THF produced in 38% yield the previously unknown *closo*-phosphacarborane complex, 1-[2,4,6-$(t\text{-}Bu)_3C_6H_2$]-1-P-2,3-$(SiMe_3)_2$-2,3-$C_2B_4H_4$ (I) as an air-sensitive, white, crystalline solid. The new complex was characterized by ^1H, ^{11}B, ^{13}C, and ^{31}P NMR, IR, and mass spectroscopy. These spectroscopic data are consistent with the proposed pentagonal-bipyramidal structure, which contains 16 skeletal valence electrons.

Introduction

A group 15 atom is isoelectronic and isolobal with a CH group. Therefore, one would expect that substitution of a group 15 element for a CH group in a dicarborane would yield compounds with similar structures and comparable reactivities. Indeed, all of the group 15 elements have been inserted into monocarborane cages, and the resulting icosahedral heterocarboranes have been characterized.[1] The icosahedral geometries of these heterocarboranes are supported by the X-ray analysis of *closo*-9,10-Cl_2-1,7-$CPB_{10}H_9$.[2] Surprisingly, the chemistry of the C_2B_9 carborane system containing group 15 elements has been limited to aza- and arsacarboranes. However, none of the group 15 elements has been incorporated into a C_2B_4 carborane as an integral part of the polyhedron. Even though Wallbridge and co-workers have reported in 1979 a brief account of the insertion of a "bare" phosphorus atom into the open face of a C_2B_8 carborane to produce *nido*-9-P-7,8-$C_2B_8H_{11}$,[3] the insertions of RP (R = aryl or alkyl group) moieties in an η^5-fashion into the dicarborane systems to produce the corresponding *closo*-phosphacarborane derivatives have not been reported to date. We report herein the synthesis and characterization of the first *closo*-phosphacarborane based on a dicarborane system.

Experimental Section

Materials. 2,3-Bis(trimethylsilyl)-2,3-dicarba-*nido*-hexaborane(8) was prepared by the methods of Hosmane et al.[4,5] Solution of the lithium sodium double salt of the *nido*-carborane dianion $Na^+(THF)Li^+[2,3\text{-}(SiMe_3)_2\text{-}2,3\text{-}C_2B_4H_4]^{2-}$ in tetrahydrofuran (THF) was prepared by the method described elsewhere.[6] The supermesityldichlorophosphine 2,4,6-$(t\text{-}Bu)_3C_6H_2PCl_2$ was prepared and purified according to the literature method.[7] The purity of the phosphorus reagent was checked by IR and NMR spectroscopy and on the basis of the melting point. A 1.7

†Southern Methodist University.
‡The University of Texas at Austin.

(1) Hosmane, N. S.; Maguire, J. A. *Adv. Organomet. Chem.* **1990**, *30*, 99.
(2) Wong, H. S.; Lipscomb, W. N. *Inorg. Chem.* **1975**, *14*, 1350.
(3) Colquhoun, H. M.; Greenhough, T. J.; Wallbridge, M. G. H. *J. Chem. Res. Synop.* **1979**, 248.
(4) Hosmane, N. S.; Sirmokadam, N. N.; Mollenhauer, M. N. *J. Organomet. Chem.* **1985**, *279*, 359.
(5) Hosmane, N. S.; Mollenhauer, M. N.; Cowley, A. H.; Norman, N. C. *Organometallics* **1985**, *4*, 1194.
(6) Siriwardane, U.; Islam, M. S.; West, T. A.; Hosmane, N. S.; Maguire, J. A.; Cowley, A. H. *J. Am. Chem. Soc.* **1987**, *109*, 4600. Barreto, R. D.; Hosmane, N. S. *Inorg. Synth.*, in press.
(7) Cowley, A. H.; Norman, N. C.; Pakulski, M. *Inorg. Synth.* **1990**, *27*, 236.

0020-1669/91/1330-1325$02.50/0